Chapter-3

Thermoelasticity under memory dependent derivative heat transfer

[1]3. Analysis of wave propagation in presence of a continuous line heat source under heat transfer with memory dependent derivatives

3.1 Introduction

The present chapter is devoted on the recently proposed concept of "memory dependent derivative" in heat transfer process in solid body. Diethelm (2010) analyzed fractional differential equations by applying the concept of Caputo fractional derivative (1967) defined as

$$D_a^{\alpha} f(t) = \int_a^t K_{\alpha}(t-\xi) f^m(\xi) d\xi \tag{3.1}$$

Here $K_{\alpha}(t-\xi)$ is denoted as kernel of function and it is defined as $K_{\alpha}(t-\xi) = \frac{(t-\xi)^{m-\alpha-1}}{\Gamma(m-\alpha)}$.

where, kernel $K_{\alpha}(t-\xi)$ is fixed; where a is a fixed integer and m is an integer such that $m-1 < \alpha < m$.

From the above definition it is clear that $\alpha-$order fractional derivative at time t is not defined locally at time t, but it depends on the total effects of $m-$order integer derivative on the interval $[a,\ t]$. Hence this concept of fractional derivative

[1]**This work has been accepted in the Journal "Mathematics and Mechanics of Solids", Jan' 2017.**

can be used to describe the variation of a system in which the instantaneous change rate depends on the past state. This is known as 'memory effect'.

However, we know that the memory effect of real process basically arises in a segment of time $[t-\tau,\, t]$, where τ denotes the time delay and it is always positive. Inspite of several applications of fractional calculus, it has some demerits. Due to this, concept of fractional order derivative has been modified and a new concept of derivative has been established by Wang and Li (2011) which has been named as 'memory dependent derivative' that can be written mathematically as

$$D^m_{\tau,K} f(t) = \frac{1}{\tau} \int_{t-\tau}^{t} K(t-s) f^m(s) ds \tag{3.2}$$

Here the choice of kernel $K(t-s)$ and time delay parameter τ can be chosen freely as the necessity of problem. For physical point of view, generally we take $0 < K(t-s) \leq 1$ and τ should be smaller than an upper bound determined by the kernel function to ensure the uniqueness and existence of the solution. Several examples like weather forecast, population model etc. need the data of recent past time and this may be possible by using the concept of memory dependent derivative since the concept of fractional order derivative fails if the value of lower terminal is very less in comparison to the value of upper terminal in the definition of fractional order derivative.

Yu *et. al* (2014) introduced memory-dependent derivative into the generalized theory of thermoelasticity provided by Lord and Shulman (1967). Furthermore Ezzat *et al.* ((2015), (2016)) introduced the concept of memory dependent derivative in magneto-thermoelasticity and generalized thermoelasticity.

We make an attempt to investigate a problem of wave propagation in a homogeneous, isotropic and unbounded solid due to a continuous line heat source and

understand the influence of memory dependent heat conduction model on the thermoelastic interaction. It must be mentioned that Prasad *et al.* (2011) presented the effects of phase lags on the propagation of wave in presence of continuous line heat source. Sherief and Anwar (1986) studied the thermoelastic interactions due to a continuous line heat source in a linear, homogeneous unbounded solid in the context of Lord-Shulman model (1967) of generalized thermoelasticity. Furthermore Temperature-rate dependent thermoelastic interactions due to a line heat source was also derived by Chandrasekharaiah and Murthy (1991). Dhaliwal *et al.* (1997) and Chandrasekharaiah and Srinath (1998) studied the generalized thermoelasticity theory of type GN-III and GN-II, respectively, to explore the theory of thermoelastic interactions generated by a continuous line heat source in a homogeneous isotropic unbounded solid.

Here, we formulate the present problem by modifying the basic governing equations in the frame of memory dependent derivative heat conduction law. We employ the potential function approach together with the Laplace and Hankel transform technique to derive the solutions in the transformed domain. Hankel inversion is performed analytically, and we achieve analytical solutions of displacement, temperature and stresses in Laplace transform domain. These results are effected by kernel function and time delay parameter.The analytical results are illustrated with numerical computation and graphical plots of distribution of the field variables for copper material. We have attempted to exhibit the significance of kernel function and time-delay parameter that are characteristics of memory dependent derivative heat transfer in the behavior of field variables with the help of numerical results. Detailed comparative analysis is presented through the numerical results to estimate the effects of the kernels and time-delay parameter on behavior of all of the field variables in presence of a heat source in the medium.

3.2 Problem formulation and governing equations

We assume a homogeneous, unbounded, thermoelastic solid which contains a continuous line heat source. Line of action of the heat source is taken along the x_3-axis. Hence the thermoelastic interactions are symmetric about the axis in nature. Due to this property of the media, temperature and the displacement are taken as $T = T(r, t)$ and $u = u(r, t)$ where r denotes the distance measured from the axis. Since media has been characterized in such a manner that the thermoelastic deformations are symmetric about the axis; hence we obtain only two components of stress tensor radial stress σ_{rr} and circumferential stress $\sigma_{\theta\theta}$. Both stresses are the components of normal stress. The basic governing equations are considered as follows:

Equation of motion:

$$\sigma_{ij,j} = \rho\ddot{u}_i \tag{3.3}$$

where $\sigma_{ij} = \lambda\Delta\delta_{ij} + 2\mu_{ij} - \gamma(T - T_0)\delta_{ij}$

ρ denotes the mass density of the material, σ_{ij} represents the components of stress tensor. $\triangle$ denotes dilatation.

Derivation of heat conduction equation using memory dependent derivative with time-delay:

Applying the concept of generalized thermoelasticity, the relation between heat flux vector $\overrightarrow{q}$ and temperature gradient vector $\overrightarrow{\nabla}T$ can be written as

$$\overrightarrow{q}(\overrightarrow{x}, t + \omega) = -K\overrightarrow{\nabla}T \tag{3.4}$$

where $\overrightarrow{x}$ is the position vector, K is thermal conductivity and ω is time-delay.

Heat conduction equation (Biot (1956)) with heat source is given by

$$\frac{\partial}{\partial t}(\rho C_e T(\overrightarrow{x},t)+\gamma T_0 e(\overrightarrow{x},t)) = -\overrightarrow{\nabla}.\overrightarrow{q}(\overrightarrow{x},t)+Q(\overrightarrow{x},t) \tag{3.5}$$

where $Q(\overrightarrow{x},t)$ denotes the heat source .

Ezzat *et al.* (2015, 2016) developed a new energy equation with memory dependent derivative having time-delay ω as

$$\overrightarrow{q}(\overrightarrow{x},t)+\omega D_\omega \overrightarrow{q}(\overrightarrow{x},t) = -K\overrightarrow{\nabla}T \tag{3.6}$$

Now using relation (3.4) and (3.6), we achieve the generalized heat conduction law for the considered new generalized theory with time-delay as

$$\overrightarrow{q}(\overrightarrow{x},t+\omega) = \overrightarrow{q}(\overrightarrow{x},t)+\omega D_\omega \overrightarrow{q}(\overrightarrow{x},t) \tag{3.7}$$

Taking the memory-time-derivative of equation (3.5), we achieve

$$\frac{\partial}{\partial t} D_\omega(\rho C_e T+\gamma T_0 e) = -\overrightarrow{\nabla}.D_\omega \overrightarrow{q}+D_\omega Q \tag{3.8}$$

Multiplying equation (3.8) by ω and then adding to equation (3.5), we obtain

$$(1+\omega D_\omega)(\rho C_e \frac{\partial}{\partial t}T+\gamma T_0 \frac{\partial e}{\partial t}) = -\overrightarrow{\nabla}.(\overrightarrow{q}+\omega D_\omega \overrightarrow{q})+(1+\omega D_\omega)Q \tag{3.9}$$

Finally, using equation (3.6) in equation (3.9), we get

$$(1+\omega D_\omega)(\rho C_e \frac{\partial}{\partial t}T+\gamma T_0 \frac{\partial e}{\partial t}) = K\nabla^2 T+(1+\omega D_\omega)Q \tag{3.10}$$

where

$$D_\omega f(t) = \frac{1}{\omega} \int_{t-\omega}^{t} K(t-s) f'(s) ds \tag{3.11}$$

Here, $f'(s)$denotes the first derivative of $f(s)$.

Equation (3.10) is therefore the generalized heat conduction equation, taking into account the memory dependent derivative with time-delay ω. We will deal equation (3.10) as the equation of heat conduction for the present study.

Since we are considering axisymmetric thermoelastic deformations, the physical fields are dependent on time variable t and the coordinates (r, θ); hence the governing equations describing our system are given as following:

Equation of motion: (obtained from eq. (3.3))

$$\mu \nabla^2 u - \frac{\mu}{r^2} u + (\lambda + 2\mu) \frac{\partial e}{\partial r} - \gamma \frac{\partial T}{\partial r} = \rho \frac{\partial^2 u}{\partial t^2} \tag{3.12}$$

Equation of heat conduction:

$$(1 + \omega D_\omega)(\rho C_e \frac{\partial}{\partial t} T + \gamma T_0 \frac{\partial e}{\partial t}) = K \nabla^2 T + (1 + \omega D_\omega) Q \tag{3.13}$$

3.3 Non-dimensional form of governing equations

In order to obtain the non-dimensional form of equations (3.12) and (3.13) we introduce the following quantities :

$u' = c_0 \eta u$, $t' = c_0^2 \eta t$, $r' = c_0 \eta r$, $\theta = \frac{T - T_0}{T_0}$, $K = \frac{\rho C_v}{\eta}$, $a_1 = \frac{\gamma T_0}{(\lambda + 2\mu)}$; $\lambda_1 = \frac{\lambda + 2\mu}{\lambda}$;

$Q' = \frac{\gamma Q}{c_0^2 \eta C_v(\lambda+2\mu)}$, $\sigma'_{rr} = \frac{\sigma_{rr}}{(\lambda+2\mu)}$,$\sigma'_{\theta\theta} = \frac{\sigma_{\theta\theta}}{(\lambda+2\mu)}$, $a_2 = \frac{\gamma}{\rho C_v}$, $c_0^2 = \frac{\lambda+2\mu}{\rho}$

$$\nabla^2\phi - a_1\theta = \frac{\partial^2\phi}{\partial t^2} \tag{3.14}$$

where we have introduced the thermoelastic potential function ϕsuch that $u = \frac{\partial\phi}{\partial r}$

$$\nabla^2\theta = (1+\omega D_\omega)(\dot{\theta} + a_2\frac{\partial}{\partial t}(\nabla^2\phi) - \frac{Q}{a_1}) \tag{3.15}$$

where we have assumed kernel such as

$$K(t-\xi) = a + b(t-\xi) \tag{3.16}$$

with a, b are real constants.

Equations (3.14) and (3.15) are the non-dimensional form of equations (3.12) and (3.13).

Now we take three different cases of the kernel function such that

Case-1: $K(t-\xi) = 1/2$; $a = 1/2, b = 0$

Case-2: $K(t-\xi) = 1/2 - (t-\xi)/\omega$; $a = 1/2, b = -\frac{1}{\omega}$

Case-3: $K(t-\xi) = 1 - (t-\xi)$; $a = 1, b = -1$

Equation (3.3) derives the components of stress as

$$\sigma_{rr} = \frac{\partial u}{\partial r} + \lambda_1\frac{u}{r} - a_1\theta \tag{3.17}$$

$$\sigma_{\theta\theta} = \lambda_1\frac{\partial u}{\partial r} + \frac{u}{r} - a_1\theta \tag{3.18}$$

As we have assumed that the heat source acting on the present media is of continuous line type, so we take it in the following form:

$$Q = \frac{1}{2\pi r} Q_0 \delta(r) H(t) \tag{3.19}$$

where Q_0 is constant, $\delta(r)$ is the Dirac delta function and $H(t)$ is the Heaviside unit step function.

Initial and boundary conditions:

We assume that all field variables vanish at $r \to \infty$. Mathematically we can write $(u, \theta, \sigma_{rr}, \sigma_{\theta\theta}) \to 0$ as $r \to \infty$.

Initial conditions are considered to be homogeneous i.e., $u = \dot{u} = \theta = \dot{\theta} = 0$ at $t = 0$.

3.4 Solution in Laplace transform domain

In the present section, we attempt to find the solution of the problem in the Laplace transform domain. Taking Laplace transform of equation (3.16) for all three different kernels, respectively we achieve

Case-1: $K(t-\xi) = 1/2$; $a = 1/2, b = 0$

$$L(\omega D_\omega(f(t))) = \frac{(1 - e^{-s\omega})}{2} f(s) \tag{3.20}$$

where $f(s)$ is the Laplace transform of $f(t)$.

Case-2: $K(t-\xi) = 1/2 - (t-\xi)/\omega$; $a = 1/2, b = -\frac{1}{\omega}$

$$L(\omega D_\omega(f(t))) = [\frac{(1 - e^{-s\omega})}{2} - \frac{(1 - e^{-s\omega})}{\omega s} + e^{-s\omega}] f(s) \tag{3.21}$$

Case-3: $K(t-\xi) = 1 - (t-\xi)$; $a = 1, b = -1$

$$L(\omega D_\omega(f(t))) = [(1 - e^{-s\omega}) - \frac{(1 - e^{-s\omega})}{s} + \omega e^{-s\omega}] f(s) \tag{3.22}$$

In general $L(\omega D_\omega(f(t)))$ can be written as:

$$G = L(\omega D_\omega(f(t))) = \frac{(as+b)(1-e^{-s\omega})}{s} - b\omega e^{-s\omega} \tag{3.23}$$

On taking Laplace transform of equations (3.14) and (3.15), we reach at the following equations, respectively:

$$\nabla^2\overline{\phi} - a_1\overline{\theta} = s^2\overline{\phi} \tag{3.24}$$

$$\nabla^2\overline{\theta} = (1+G)(s\overline{\theta} + a_2 s(\nabla^2\overline{\phi}) - \frac{\overline{Q}}{a_1}) \tag{3.25}$$

where $\overline{Q}$ can be determined as

$$\overline{Q} = \frac{1}{2\pi r s} Q_0 \delta(r) \tag{3.26}$$

As equations (3.23) and (3.24) are coupled with the field variables $\overline{\phi}$ and $\overline{\theta}$, eliminating $\overline{\theta}$ between equations (3.24) and (3.25), we obtain the following equation of order four:

$$\nabla^4\overline{\phi} - [s^2 + (1+G)(1+\epsilon)s]\nabla^2\overline{\phi} + (1+G)s^3\overline{\phi} = -\frac{Q_0\delta(r)(1+G)}{2s\pi r} \tag{3.27}$$

where $\epsilon = a_1 a_2$

Equation (3.27) can be rewritten as

$$(\nabla^2 - m_1^2)(\nabla^2 - m_2^2)\bar{\phi} = -\frac{Q_0\delta(r)(1+G)}{2s\pi r} \tag{3.28}$$

where m_1 and m_2 are the roots of the equation given below:

$$m^4 - [s^2 + (1+G)(1+\epsilon)s]m^2 + (1+G)s^3 = 0 \tag{3.29}$$

In order to solve equation (3.28), we use Hankel transform which can be defined as

$$\hat{f}(\xi, s) = \int_0^\infty r J_0(\xi r) \bar{f}(r, s) dr \tag{3.30}$$

where J_0 is the Bessel function of first kind and of zero order.

Applying Hankel transform in equation (3.28), we obtain

$$(\xi_1^2 + m_1^2)(\xi_2^2 + m_2^2)\hat{\phi} = -\frac{Q_0(1+G)}{2s\pi} \tag{3.31}$$

Further, we apply Inverse Hankel transform which can be written as

$$\overline{f}(\xi, s) = \int_0^\infty \xi J_0(\xi r) \hat{f}(\xi, s) d\xi \tag{3.32}$$

Applying Inverse Hankel transform in equation (3.31) we achieve

$$\overline{\phi}(r, s) = \frac{Q_0(1+G)[\sum_{i=1}^{2}(-1)^{i-1}[K_0(m_i r)]]}{2\pi s(m_1^2 - m_2^2)} \tag{3.33}$$

Here $K_0(m_i r)$ is the modified Bessel function of the second kind and of order 0.

Using equation (3.33) in the expression $u = \frac{\partial \phi}{\partial r}$, we achieve the following analytical solution of displacement in Laplace transform domain:

$$\bar{u}(r, s) = \frac{Q_0(1+G)[\sum_{i=1}^{2}(-1)^{i-1}[-m_i K_1(m_i r)]]}{2\pi s(m_1^2 - m_2^2)} \tag{3.34}$$

Further, with the help of equation (3.24), we achieve the following analytical result of temperature in the Laplace transform domain:

$$\bar{\theta}(r,s) = \frac{Q_0(1+G)[\sum_{i=1}^{2}(-1)^{i-1}[(m_i - s^2)K_0(m_i r)]]}{2\pi s a_1(m_1^2 - m_2^2)} \tag{3.35}$$

Now, taking Laplace transform of equations (3.17) and (3.18), we obtain the following stresses in Laplace transform domain

$$\overline{\sigma}_{rr} = [\frac{(\lambda_1 - 1)}{r}\frac{\partial}{\partial r} + s^2]\overline{\phi} \tag{3.36}$$

$$\overline{\sigma}_{\theta\theta} = [\frac{(\lambda_1 - 1)}{r}\frac{\partial^2}{\partial r^2} + s^2]\overline{\phi} \tag{3.37}$$

Substituting analytical result of $\overline{\phi}$ in equations (3.36) and (3.37), we obtain the following solutions of the components of normal stress:

$$\bar{\sigma}_{rr}(r,s) = \frac{Q_0(1+G)[\sum_{i=1}^{2}(-1)^{i-1}[(1-\lambda_1)m_i K_1(m_i r) + r s^2 K_0(m_i r)]]}{2\pi s r(m_1^2 - m_2^2)} \tag{3.38}$$

$$\bar{\sigma}_{\theta\theta}(r,s) = \frac{Q_0(1+G)[\sum_{i=1}^{2}(-1)^{i-1}[r((\lambda_1 - 1)m_i^2 + s^2)K_0(m_i r) + (\lambda_1 - 1)m_i K_1(m_i r)]]}{2\pi s r(m_1^2 - m_2^2)} \tag{3.39}$$

where, $K_1(m_i r)$ is the modified Bessel function of second kind and of order one. Here, we have used the following recurrence relations for modified Bessel function of second kind:

$\frac{\partial}{\partial r}K_0(r) = -K_1(r)$ and $\frac{\partial}{\partial r}[rK_1(r)] = -rK_0(r)$

Equations [(3.34), (3.35), (3.38) and (3.39)] constitute the solution of the present system in the Laplace transform domain.

The solution in the present domain can be obtained by inverting the Laplace

transforms involved in the solutions (3.34), (3.35), (3.38), (3.39). It is a formidable task to find the inverse Laplace transforms of equations (3.34), (3.35), (3.38), (3.39) analytically for all values of time due to the participation of the complicated expressions given above on the Laplace transform parameter, s. Hence, in order to analyze the influence of different kernel functions and time delay in the nature of all physical fields such as temperature, displacement and radial and circumferential stresses, we obtain numerical results which have been discussed in the next section.

3.5 Numerical results and discussions

In order to demonstrate the theoretical results obtained in the previous section and to unveil the consequence of using memory dependent derivative in our field variables - temperature, displacement and normal stresses, we assume that $Z = a_1\theta$ and $Q_0 = 1$. we carry out numerical work with the help of computer programming using the software Mathematica. For this purpose, we consider the copper material, and the physical data are taken as (Chandrasekharaiah and Srinath (1998): $\epsilon = 0.0168$, $\lambda = 7.76 \times 10^{10} Nm^{-2}$, $\mu = 3.86 \times 10^{10} Nm^{-2}$, $C_v = 383.1 J/KgK$, $\rho = 8954 kg/m^3$, $T_0 = 293K$

Here, we employ the numerical method proposed by Bellmen *et al.* (1966) for the inversion of Laplace transforms, and compute the numerical values of these physical quantities by directly solving equations (3.34), (3.35), (3.38), (3.39) numerically. We compute the numerical values of temperature, displacement, radial stress and circumferential stress at three different non-dimensional times ($t = 0.35$, 0.69 and 1.21) by using the solutions given by equations (3.34), (3.35), (3.38) and (3.39). In the present section, we have attempted to show the effect of kernel function as well as time delay among the nature of all physical fields temperature, displacement and both radial and circumferential stresses.

3.5.1 Behavior of temperature

The variation of temperature field has been shown in two ways - firstly when kernel functions are different but time delay parameter is fixed and secondly for a particular kernel function but for different values of time delay. Figure 3.1 shows the distribution of temperature at three non-dimensional times 0.35, 0.69 and 1.21 and for time delay $\omega = 0.1$. The computations are performed for different forms of kernel function namely $K(t,\xi) = \frac{1}{2}$, $K(t,\xi) = \frac{1}{2} - \frac{(t-\xi)}{\omega}$ and $K(t,\xi) = 1 - (t-\xi)$. The region of influence for temperature is clearly indicated to be finite in all cases. It is noted that temperature field has the maximum value at initial point i.e. when the distance $r = 0$. Further, after some distance temperature field is observed to show one local minimum value and thereafter one local maximum value before it vanishes out completely. This field has decreasing trend as the distance increases. The positions of extreme points shift towards right with the increase of time. We also see that the temperature attains its highest value when the kernel function is taken as $(1 - (t - \xi))$ and lowest value for the constant kernel function, i.e. when $K(t,\xi) = \frac{1}{2}$ for a particular time. Hence, we note that kernel function plays significant role in the variation of temperature and the influence of kernel is observed to be more prominent near the vicinity of extreme points at all times. Further it is also noted that the effect of kernel function is more prominent at small time. Figure 3.2 represents nature of temperature for the case of constant kernel function $(K(t,\xi) = \frac{1}{2})$ for different time delays, i.e., for ω =0.01, 0.05 and 0.1 at three non dimensional times 0.35, 0.69 and 1.21. The variation of temperature with time delay parameter for the linear kernel function is displayed in Figure 3.3. From Figures 3.2 and 3.3, we note that the effect of time delay in the behavior of temperature is significant. The effect is more prominent for linear kernel function as compared to

constant kernel function. There is one local maximum value followed by one local minimum value of temperature in each case. However, the extreme values are shifted towards right as time increases and the region of influence also increases with the increase of time. However, the region of influence increases with the decrease of time delay parameter. It is observed that the effect of time delay is more significant at initial time.

3.5.2 Behavior of displacement

Figure 3.4 presents the variation of displacement at three non-dimensional times 0.35, 0.69 and 1.21 for different kernel functions but when time delay parameter ω is fixed and its value is 0.1. Computations are performed for three different kernel functions namely $(K(t,\xi) = \frac{1}{2})$, $(K(t,\xi) = \frac{1}{2} - \frac{(t-\xi)}{\omega})$ and $(K(t,\xi) = 1-(t-\xi))$. Here we observe that there is no local minimum. Only local maximum is present in the profiles. The trend of variation is in such a manner that it starts from a very small value and then slowly increases. After gaining a peak value it goes down. In the present profiles, we see that the influence of kernel function is very much prominent and this influence decreases as the time decreases. Moreover it is also observed that the kernel function is more effective at the vicinity of local maximum at all times. The region of influence increases as the time increases. Local maximum attains its highest value for the linear kernel function $K(t,\xi) = 1-(t-\xi)$ and lowest value for the kernel function $K(t,\xi) = \frac{1}{2} - \frac{(t-\xi)}{\omega}$ at all three times. Figure 3.5 and 3.6 show the variation of displacement at different values of time delay $\omega = 0.01,\ 0.05,\ 0.1$ but for fixed kernel functions $K(t,\xi) = \frac{1}{2}$ and $K(t,\xi) = 1-(t-\xi)$, respectively. The pattern of variation of displacement is same as Figure 3.4. However, we observe the influence of ω in each profile at all times and this influence is more prominent near local maximum value. Region of influence increases as time increases. Local

maximum is of highest value for $\omega = 0.1$ and is of lowest value for $\omega = 0.01$. It is also noted that the effect of time delay parameter ω is more prominent for the linear kernel function $K(t, \xi) = (1 - (t - \xi))$.

3.5.3 Behavior of stresses

3.5.3.1 Behavior of radial stress

Figure 3.7 represents the variation of radial stress with distance r for different kernel functions $(K(t, \xi) = \frac{1}{2})$, $(K(t, \xi) = \frac{1}{2} - \frac{(t-\xi)}{\omega})$ and $(K(t, \xi) = 1 - (t - \xi))$ at constant time delay $\omega = 0.1$ for non-dimensional times 0.35, 0.69 and 1.21. The trend of variation for the present profile is in such a way that it starts from a negative value and goes towards positive direction and ultimately becomes vanish. Here we observe that firstly we achieve a local maximum and then local minimum value in the variation of radial stress in each case. Effect of kernel function is prominent in each profile and this influence is very significant at the vicinity of local maximum and local minimum values. Further, it should be pointed out that the local maximum attains its lowest numerical value for the linear kernel function $(K(t, \xi) = 1 - (t - \xi))$and the highest numerical value for the kernel function $K(t, \xi) = \frac{1}{2} - \frac{(t-\xi)}{\omega}$. The Region of influence increases as the time increases. Figures 3.8 and 3.9 show the trend of variation of radial stress for particular kernel functions namely, $K(t, \xi) = \frac{1}{2}$, and $K(t, \xi) = 1-(t-\xi)$, respectively but for different values of time delay ω at three non-dimensional times 0.35, 0.69 and 1.21. Pattern of variation of radial stress is similar in nature like the variation observed from Figure 3.7. One local maximum and then one local minimum value is attained by each plot and the stress is compressive in nature. Effect of time delay ω is very much significant near extreme points. Furthermore it is observed that time delay is more effective among the profiles of radial stress for linear kernel function i.e. $(K(t, \xi) = 1 - (t - \xi))$. Local maximum

and local minimum achieve their higher numerical value for time delay $\omega = 0.1$. Here we can conclude that as time delay increases, we obtain higher value of local maximum of the present profile. The region of influence is directly proportional to time; it means that region of influence increases with the increment of time.

3.5.3.2 Behavior of circumferential stress

Figure 3.10 depicts the behavior of circumferential stress for different kernel functions -($K(t,\xi) = \frac{1}{2}$), ($K(t,\xi) = \frac{1}{2} - \frac{(t-\xi)}{\omega}$) and ($K(t,\xi) = 1 - (t-\xi)$) at constant time delay $\omega = 0.1$ for non-dimensional times 0.35, 0.69 and 1.21. We observe one local maximum and one local minimum in the distributions of circumferential stress. Influence of kernel function is more prominent at the vicinity of extreme points. As in the case of radial stress, the region of influence is directly proportional to time for this field too. Here local maximum occurs with its highest numerical value for the kernel function, $K(t,\xi) = \frac{1}{2} - \frac{(t-\xi)}{\omega}$ and with its lowest value for the kernel function $K(t,\xi) = 1 - (t-\xi)$. Figures 3.11 and 3.12 present the nature of circumferential stress for kernel functions $K(t,\xi) = \frac{1}{2}$, and $K(t,\xi) = 1 - (t-\xi)$, respectively. However, we have taken different values of time delay ω in Figure 3.11 and 3.12. The nature of the variation of the present field for different values of time delay is same as the variation shown in Figure 3.10. But in this case local maximum attains its highest numerical value for the linear kernel function (i.e., when $K(t,\xi) = 1-(t-\xi)$) and the lowest value for the constant kernel function i.e.($K(t,\xi) = \frac{1}{2}$). The region of influence increases with the increase of time for this field too.

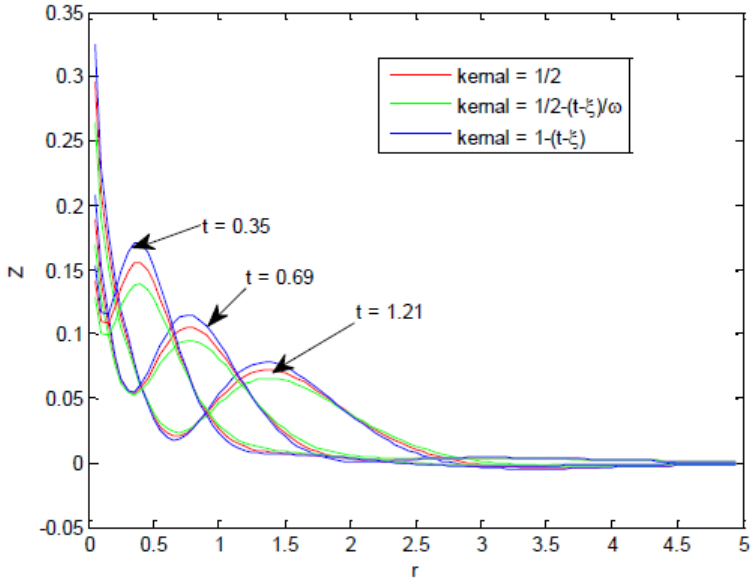

Figure 3.1 Variation of temperature distribution for time delay, $\omega = 0.1$

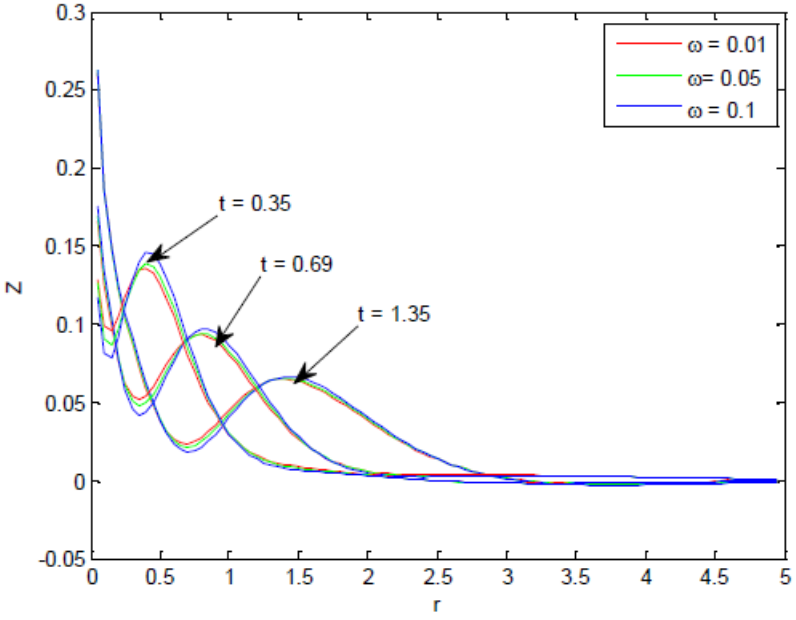

Figure 3.2 Variation of temperature distribution for kernel function, $K(t, \xi) = \frac{1}{2}$

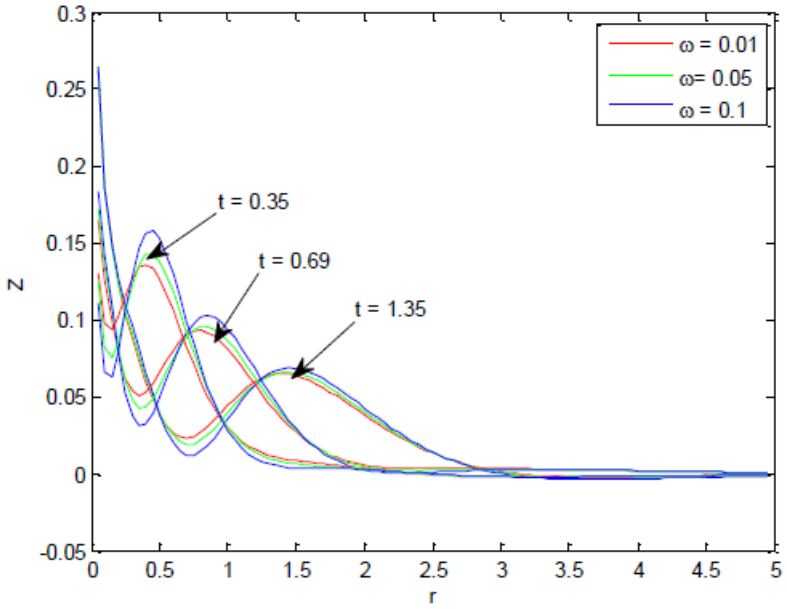

Figure 3.3 Variation of temperature distribution for kernel function, $K(t,\xi) = (1-(t-\xi))$

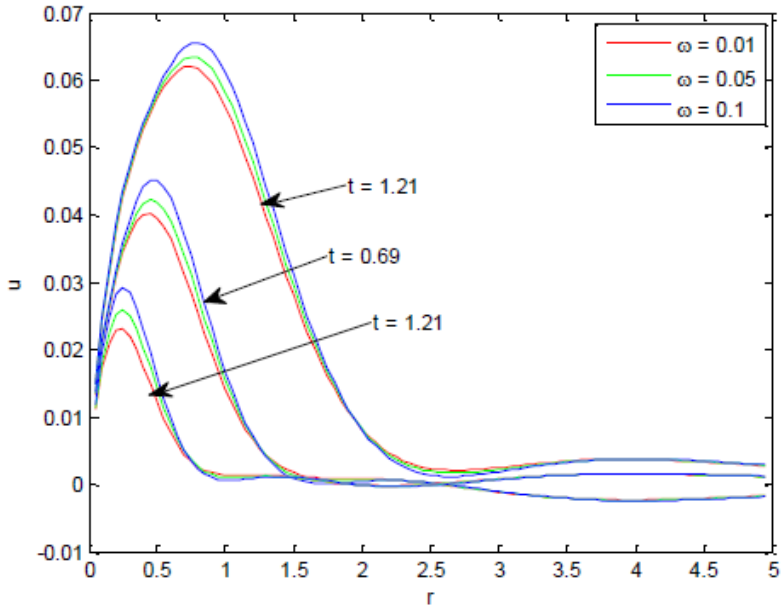

Figure 3.4 Variation of displacement for time delay, $\omega = 0.1$

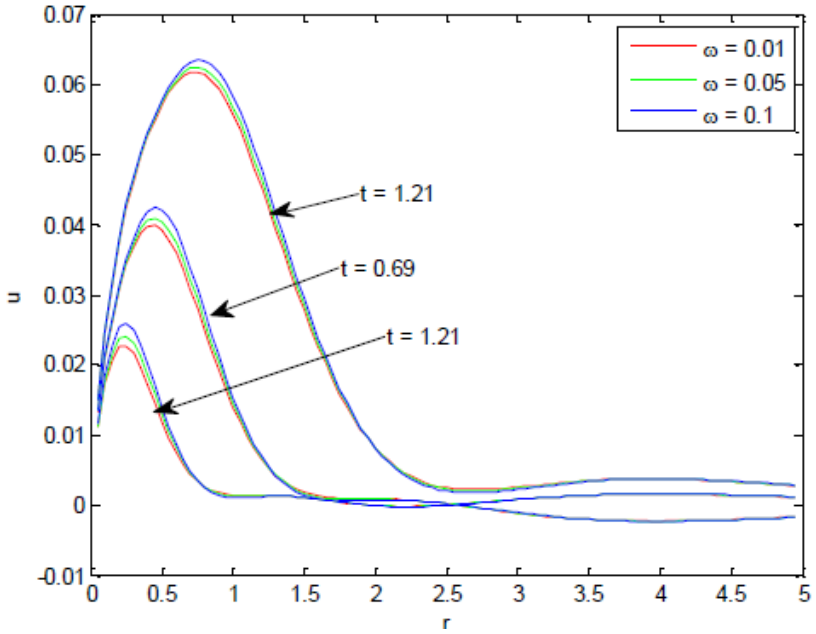

Figure 3.5 Variation of displacement for kernel function, $K(t,\xi) = \frac{1}{2}$

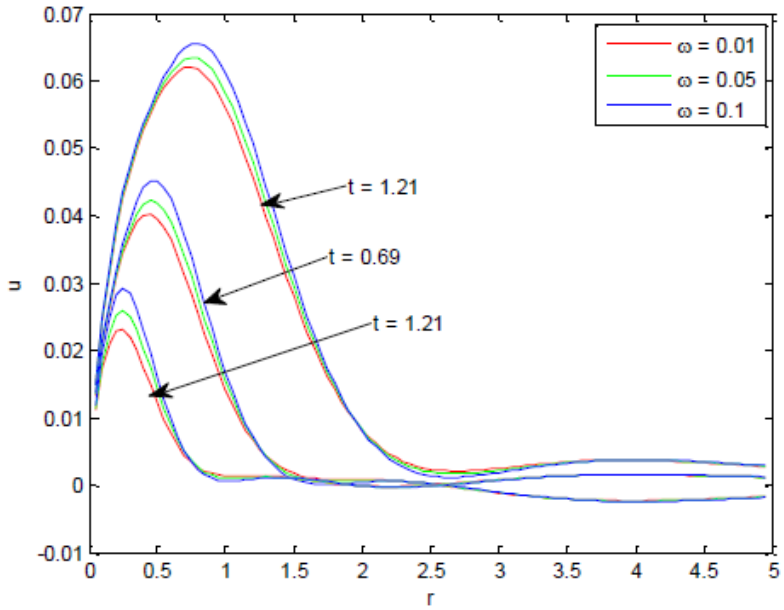

Figure 3.6 Variation of displacement for kernel function, $K(t,\xi) = (1-(t-\xi))$

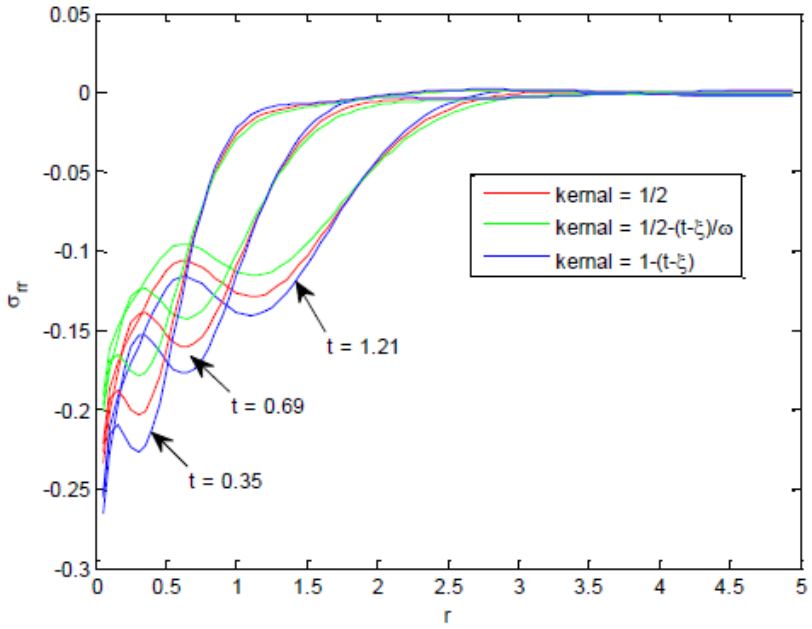

Figure 3.7 Variation of radial stress for time delay, $\omega = 0.1$

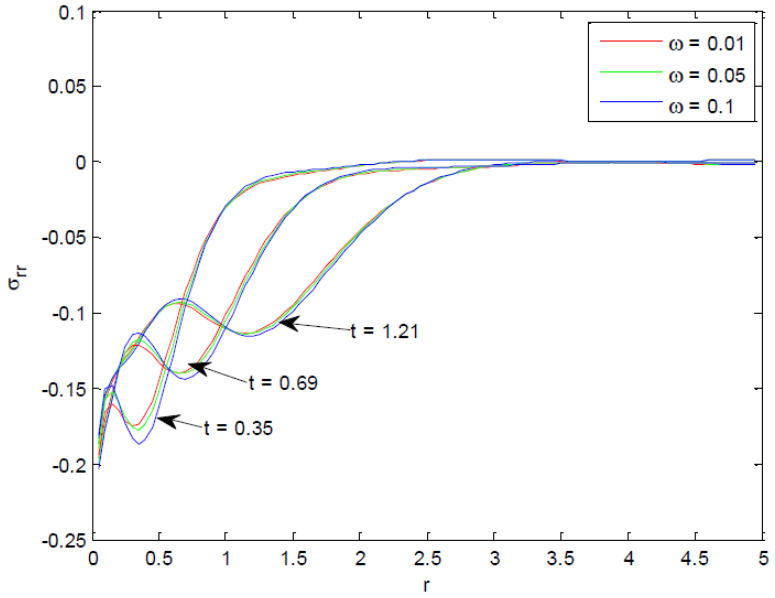

Figure 3.8 Variation of radial stress for kernel function, $K(t, \xi) = \frac{1}{2}$

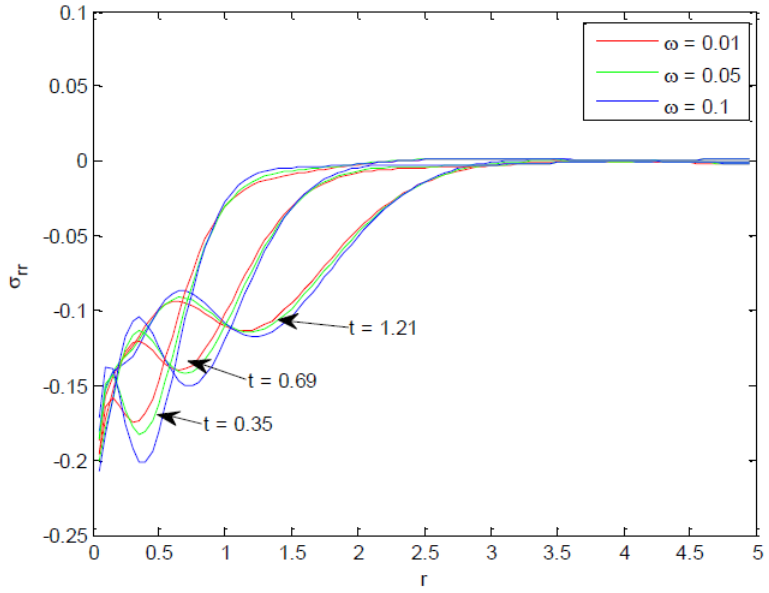

Figure 3.9 Variation of radial stress for kernel function, $K(t,\xi) = (1-(t-\xi))$

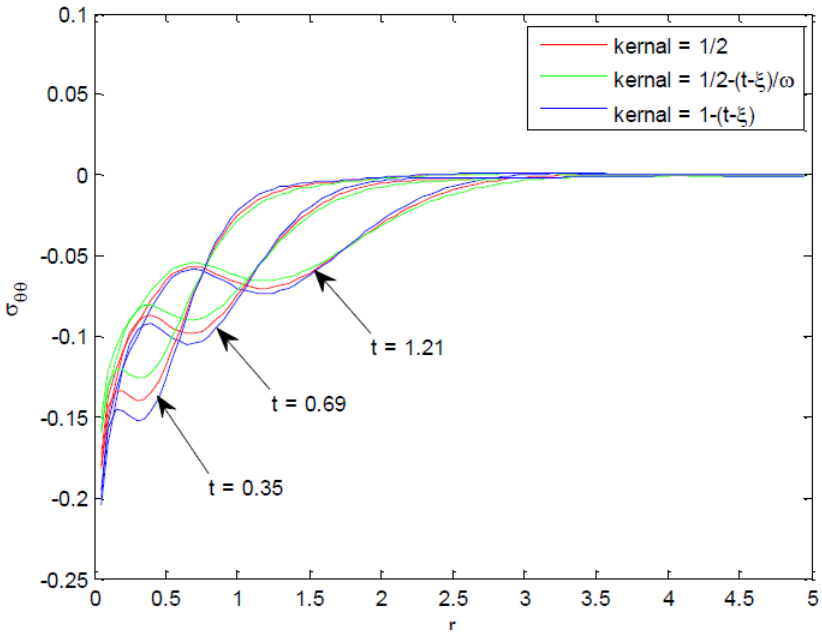

Figure 3.10 Variation of circumferential stress for time delay, $\omega = 0.1$

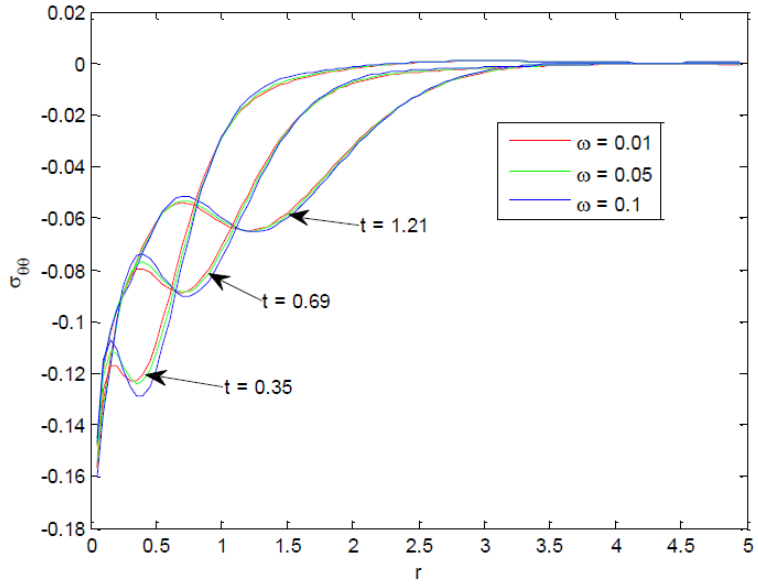

Figure 3.11 Variation of circumferential stress for kernel function, $K(t,\xi) = \frac{1}{2}$

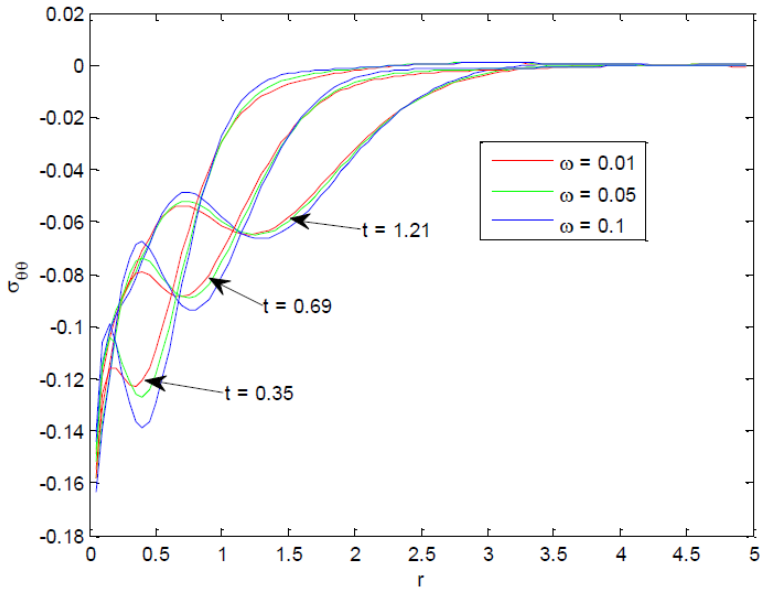

Figure 3.12 Variation of circumferential stress for kernel function, $K(t,\xi) = (1-(t-\xi))$

3.6 Conclusions

The present section represents the brief essence of the present work as well as the influence of the presence of memory dependent derivative in the heat conduction equation. Significance of chosen kernel and time delay on cylindrical wave propagation in a homogeneous, isotropic and unbounded solid due to a continuous line heat source have been investigated by employing the theory of thermoelasticity with memory dependent derivatives. After obtaining the analytical results of the physical fields like temperature, displacement and normal stresses - radial stress and circumferential stress in Laplace transform domain, numerical computation has been performed by taking a copper-like material, and the theoretical predictions are emphasized by different figures. Behavior of all physical fields for the present problem are exhibited by taking two different cases-firstly when kernel functions are different and the time delay is fixed and secondly when the kernel is fixed but time delay parameter varies. The following points are concluded from the present work:

1. Each solution consists of the combination of two coupled waves namely elastic mode wave and thermal mode wave.

2. Distributions of temperature, radial stress and circumferential stress contains local maximum and local minimum values however displacement is free from any local minimum.

3. Effect of kernel function can be observed everywhere among the profiles of physical fields. This effect is more prominent in the profiles of displacement.

4. Effect of kernel is more prominent at the vicinity of extreme points in each case.

5. Radial stress starts from a high negative value in comparison to circumferential stress in each case.

6. Time delay parameter ωalso plays a significant role in the behavior of all physical fields and it is more prominent near the vicinity of extreme points. While observing the influence of time delay ω in the variation of physical fields, we always obtain local maximum attaining its highest absolute value for the case of kernel function, $K(t, \xi) = 1 - (t - \xi)$.

7. Region of influence for each physical field is directly proportional to time implying that region of influence increases as the time increases.

8. The main objective of this work is to introduce a unified new model of thermoelasticity theory with time delay and kernel function by using the definition for reflecting the memory effect as well as importance of kernel function and time delay. We note that at any time, the region of influence for each field is finite for any kernel function or any time delay parameter. This implies that the present theory of thermoelasicity with memory dependent time derivatives supports for the finite speed of waves propagating through the medium for any thermoelastic interaction. Hence, this theory is indeed a generalized theory of thermoelasticity.